

Resonant terahertz response of a slot diode with a two-dimensional electron channel

© V.V. Popov[¶], G.M. Tsymbalov, M.S. Shur^{*}, W. Knap^{*+}

Institute of Radio Engineering and Electronics (Saratov Division), Russian Academy of Sciences,
410019 Saratov, Russia

^{*} Department of Electrical, Computer, and System Engineering and RPI/IBM Center for Broadband Data Transfer,
CII9015, Rensselaer Polytechnic Institute,

Troy, New York, 12180

⁺ GES CNRS-Universite Montpellier2 UMR 5650,
34900 Montpellier, France

(Получена 1 июня 2004 г. Принята к печати 14 июня 2004 г.)

Terahertz response of a slot diode with two-dimensional electron channel is calculated on the basis of the first principles of electromagnetism. It is shown that all characteristic electromagnetic lengths (scattering, absorption and extinction lengths) as well as the impedance of the diode exhibit resonances at the frequencies of plasmon excitation in the channel. The fundamental resonance behaves similar to the current resonance in a *RLC* circuit. A conclusion is drawn that a slot diode with two-dimensional electron channel provides a resonant circuit at terahertz frequencies that couples effectively to external electromagnetic radiation with loaded *Q*-factor exceeding unity even at room temperature. The diode resistance may be measured from contactless measurements of the characteristic electromagnetic lengths of the diode.

1. Introduction

High-frequency response of field-effect transistors and diodes with two-dimensional electron channels is strongly affected by plasma oscillations in the channel. This phenomenon in its various manifestations can be used for the detection, frequency multiplication and generation of terahertz (THz) radiation [1–13]. One of the main parameters of a device, which determines its high frequency properties, is the device impedance. The high-frequency impedance (admittance) of a slot diode was calculated for capacitively [14] and conductively [15] contacted two-dimensional electron channel in the frame of the electrostatic theory and an equivalent circuit approach. In these approaches, the radiative contribution to the impedance (radiation resistance, R_{rad} , of the diode) is not accounted for and inter-contact geometrical capacitance, C_g , is either ignored altogether [14] or treated as a free parameter [15]. However, at ultra-high (terahertz) frequencies (i) the radiation resistance of the diode may play a role as additional damping mechanism and (ii) the inter-contact geometrical capacitance may effectively shunt the channel. Furthermore, a typical length of the side contacts in high-frequency high-electron-mobility transistors (HEMT) [12] is comparable with the THz radiation wavelength, what makes the electrostatic calculations of the inter-contact capacitance inaccurate. We calculate here the impedance of a slot diode with conductively contacted two-dimensional electron channel using the full system of the Maxwell equations. In this way, we account for the radiation resistance and inter-contact capacitance from the first principles. In addition to its own practical importance, the slot diode analyzed here is an idealization of long ungated parts of the HEMT with ultra-short nanometer gate. Such HEMT was recently shown to exhibit resonant THz emission tunable by a bias voltage [12].

[¶] E-mail: popov@ire.san.ru

2. Theoretical model

Consider a plane electromagnetic wave incident normally from vacuum onto a perfectly conductive plane $z = 0$ with a slot of width w , which is located on the surface of a dielectric substrate. We assume that the electric field of the wave, $E_0 \exp(-i\omega t - ik_0 z)$, where $k_0 = \omega/c$ with c being the speed of light in vacuum, is polarised across the slot (along the x -axis). The edges of the slot are connected by a two-dimensional electron channel with the areal conductivity described by the Drude model as

$$\sigma(\omega) = i \frac{Ne^2}{m^*(\omega + i\nu)},$$

where ν is the electron momentum scattering rate, N is the sheet electron density, e and m^* are the charge and effective mass of electron, respectively.

Our theoretical procedure involves the following steps. We rewrite the Maxwell equations in the ambient medium and in the substrate in the Fourier transform representation over the in-plane wave vector k_x . The Fourier transforms of in-plane components of the electric and magnetic fields satisfy the following boundary conditions at $z = 0$:

$$\delta(k_x)E_0 + E_{x,a}^{(\text{ind})}(k_x) = E_{x,s}^{(\text{tot})}(k_x),$$

$$\delta(k_x)H_0 + H_{y,a}^{(\text{ind})} - H_{y,s}^{(\text{tot})}(k_x) = j(k_x),$$

where $j(k_x)$ is the Fourier transform of the surface electron current density, $\delta(k_x)$ is the Dirac δ -function, the subscripts a and s label the fields in the ambient medium and the substrate, respectively, and superscripts (ind) and (tot) refer to induced and total fields, E_0 and H_0 are the amplitudes of electric and magnetic fields in the incident wave. Then we relate the Fourier transform of the surface

electron current density in the diode plane to that of the in-plane electric field in the same plane as

$$j(k_x) = G(k_x)E_x(k_x) + \frac{2}{Z_0}\delta(k_x)E_0,$$

where $E_x(k_x) = E_{x,s}^{(\text{tot})}(k_x)$ is the Fourier transform of in-plane component of the total electric field in the diode plane, Z_0 is the free-space impedance. The k_x -space surface admittance $G(k_x)$ depends exclusively on the frequency and dielectric constants of the ambient medium, ϵ_a (which we assume to be 1), and the substrate, ϵ_s :

$$G(k_x) = \frac{\chi_a + \chi_s}{Z_0},$$

where

$$\chi_{a(s)} = \frac{\epsilon_{a(s)}k_0}{\sqrt{k_0^2\epsilon_{a(s)} - k_x^2}}.$$

Coming back to the real-space representation we have

$$j(x) = \frac{2E_0}{Z_0} + \int_{-\infty}^{\infty} dx' E_x(x') \int_{-\infty}^{\infty} dk_x G(k_x) \exp[ik_x(x - x')].$$

Using Ohm law $j(x) = \sigma(\omega)E_x(x)$ for the two-dimensional electron channel and the condition $E_x = 0$ for the perfectly conductive contact semi-planes, we arrive at the following integral equation for in-plane component of the total electric field within the slot:

$$\sigma(\omega)E_x(x) = \int_{-w/2}^{w/2} G(x, x')E_x(x')dx' + \frac{2E_0}{Z_0} \quad (1)$$

with the kernel

$$G(x, x') = \int_{-\infty}^{\infty} dk_x G(k_x) \exp[ik_x(x - x')].$$

Integral equation (1) is solved numerically by the Galerkin method through its projection on an orthogonal set of the Legendre polynomials within the interval $[-w/2, w/2]$. As a result we find the induced electric field in the ambient medium as

$$\mathbf{E}_a^{(\text{ind})}(\mathbf{r}) = \mathbf{E}_0 \exp(ik_0z) + \int_{-\infty}^{\infty} \mathbf{E}_a^{(\text{sc})}(k_x) \exp(i\mathbf{k}_a\mathbf{r})dk_x, \quad (2)$$

and the total electric field in the substrate as

$$\mathbf{E}_s^{(\text{tot})}(\mathbf{r}) = \int_{-\infty}^{\infty} \mathbf{E}_s^{(\text{sc})}(k_x) \exp(i\mathbf{k}_s\mathbf{r})dk_x. \quad (3)$$

The electric fields $\mathbf{E}_a^{(\text{ind})}(\mathbf{r})$ and $\mathbf{E}_s^{(\text{tot})}(\mathbf{r})$ have zero y -components and \mathbf{r} is the two-dimensional radius vector $\mathbf{r} = \{x, y\}$.

The wave vectors $\mathbf{k}_{a(s)}$ have k_x and $k_z = \pm\sqrt{k_0^2\epsilon_{a(s)} - k_x^2}$ as their components. The integrals in the right sides of Eqs. (2) and (3) describe the scattered fields in terms of the plane-wave continuum, while the first summand in Eq. (2) is the wave reflected normally from perfectly conductive plane. The sing before the radical in expression for k_z is chosen to correspond the outgoing waves for $k_x < k_0\sqrt{\epsilon_{a(s)}}$ and evanescent waves for $k_x > k_0\sqrt{\epsilon_{a(s)}}$ is respective medium.

Since only the outgoing plane waves (with $k_x < k_0\sqrt{\epsilon_{a(s)}}$) contribute to radiative losses, we can calculate the fluxes of energy scattered per unit length of the slot in each medium as

$$P_{a(s)} = \frac{\pi}{Z_0} \int_{-k_0\sqrt{\epsilon_{a(s)}}}^{k_0\sqrt{\epsilon_{a(s)}}} \mathbf{n}_{a(s)} \frac{\mathbf{k}_{a(s)}}{k_0} |\mathbf{E}_{a(s)}^{(\text{sc})}(k_x)|^2 dk_x,$$

where $\mathbf{n}_{a(s)}$ is the internal normal to the diode plane into respective medium. Then we can define the scattering length as $L_{a(s)}^{(\text{sc})} = P_{a(s)}/P_0$ in each medium, where P_0 is the energy flux density in incident wave. We can also introduce the total scattering length as $L^{(\text{sc})} = L_a^{(\text{sc})} + L_s^{(\text{sc})}$ and the absorption length $L^{(\text{ab})} = Q/P_0$, where

$$Q = \frac{1}{2} \int_{-w/2}^{w/2} |E_x(x, 0)|^2 \text{Re}[\sigma(\omega)] dx$$

is the energy absorption rate (per unit length of the slot). The scattering and absorption lengths obey the energy conservation law in the form $L^{(\text{sc})} + L^{(\text{ab})} = L^{(\text{ex})}$, where

$$L^{(\text{ex})} = 4\pi \frac{\text{Re}[\mathbf{E}_0^* \mathbf{E}_a^{(\text{sc})}(k_x = 0)]}{|E_0|^2} \quad (4)$$

is the extinction length, which is the ratio between the amount of energy picked out of the incident wave per unit time (per unit length of the slot) and the energy flux density in incident wave. The formula analogous to Eq. (4) is known as the *optical theorem* in the scattering theory [16].

3. Results and discussion

The calculated spectra of the scattering, absorption and extinction lengths are shown in Fig. 1 for parameters typical of two-dimensional electron channels in sub-100 nm gate length HEMT at room temperature [12]. All characteristic lengths exhibit maxima at frequencies of the plasmon resonances in the channel. Note that the extinction length exceeds by the order of magnitude a geometrical width of the slot even for a short electron relaxation time chosen for the calculations. Arrows in Fig. 1 mark the frequencies of ungated plasmons in isolated two-dimensional electron channel with wave vectors $q_n = (2n - 1)\pi/w$ ($n = 1, 2, 3, \dots$),

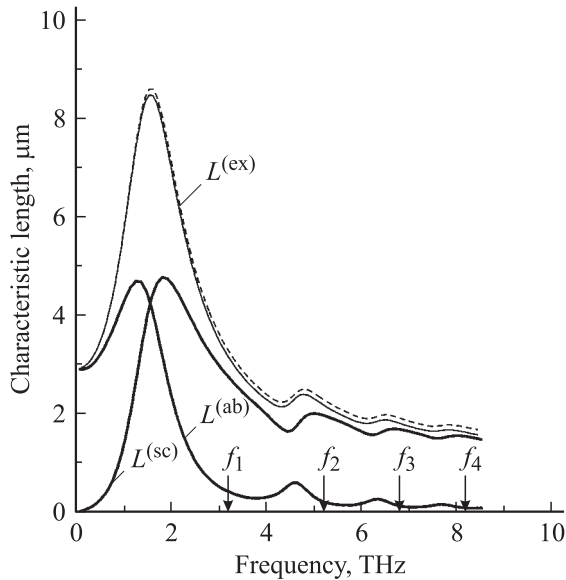


Figure 1. Characteristic lengths vs. frequency for the slot diode with parameters: $N = 3 \cdot 10^{12} \text{ cm}^{-2}$, $\nu = 4.35 \cdot 10^{12} \text{ s}^{-1}$, $w = 1.3 \mu\text{m}$, $\epsilon_s = 13.88$, $m^* = 0.042m_0$.

which are estimated by a simple approximate formula [17]:

$$f_n = \frac{1}{2\pi} \sqrt{\frac{e^2 N q_n}{m^* \epsilon_0 (1 + \epsilon_s)}}. \quad (5)$$

It is evident from Fig. 1 that the plasma oscillations in the slot diode are softened because of the induction of image charges in the perfectly conductive contact semi-planes by plasma oscillations.

In the equivalent circuit description, we can characterize the slot diode with two-dimensional electron channel by its impedance. Within the channel the total current is the sum of the electron current and displacement current caused by oscillating charges in both the channel and contacts of the diode. Far away from the slot, the current in the contact planes is purely conductive and is determined by the amplitude of incident wave. Since the total current is conserved along the circuit, we can define the diode impedance $Z = R + iX$ (per unit length of the slot) as

$$Z = \frac{1}{I} \int_{-w/2}^{w/2} E_x(x) dx,$$

where $I = 2E_0/Z_0$ is the surface current density induced by the incident wave in the perfectly conductive contact planes.

The frequency dependence of the diode normalized impedance shown in Fig. 2 displays resonances at the plasmon excitation frequencies. The reactance, X , exhibits transition from inductive ($X < 0$) behavior caused by the kinetic inductance of the electron channel to a capacitive behavior ($X > 0$) at the frequency of the fundamental plasmon resonance, which corresponds to the current resonance in the equivalent circuit description. However, no

current resonance is exhibited at higher plasmon resonant frequencies.

The normalized resistance, R/Z_0 , is, in essence, the matched width of the diode (measured along the slot), since the resistance of diode with the matched width is equal to the free-space impedance. The following *theorem* is valid: $4R = Z_0 L^{(ex)}$. The extinction length calculated using this formula (dashed curve in Fig. 1) and by Eq. (4) (solid line) coincide within the accuracy of our numerical procedure. Accordingly, we can introduce the electron resistance, R_e , and radiation resistance, R_{rad} , where $R_e = Z_0 L^{(ab)}/4$ and $R_{rad} = Z_0 L^{(sc)}/4$, respectively, so that the total resistance of the diode is given by $R = R_e + R_{rad}$. Note that R does not vanish at high frequencies (but approaches R_{rad} instead).

One can see from Fig. 2 that higher resonances are not nearly so pronounced as predicted by the electrostatic description [15] because $R_{rad} C_g$ circuit effectively shunts plasma oscillations in the channel at high frequencies. However, a sharp fundamental resonance, which corresponds to the current resonance in the equivalent circuit description, shows up even for room temperature parameters of the diode.

The frequency of the fundamental plasma resonance in the slot diode increases with decreasing the slot width (according to formula (5) it varies roughly as a square root from the inverse of the slot width). Figs. 3 and 4 exhibit absorption length and scattering length spectra for 100-nm width of the slot for different electron scattering rates. Notice that the resonant absorption (the excess of the absorption at the resonance over the non-resonant Drude background) grows considerably with decreasing the width of the slot (cf. Figs. 1 and 3). Clearly, the fundamental plasma resonance becomes narrower with decreasing the electron scattering rate. However, the width of the resonance remains finite due to the radiative damping

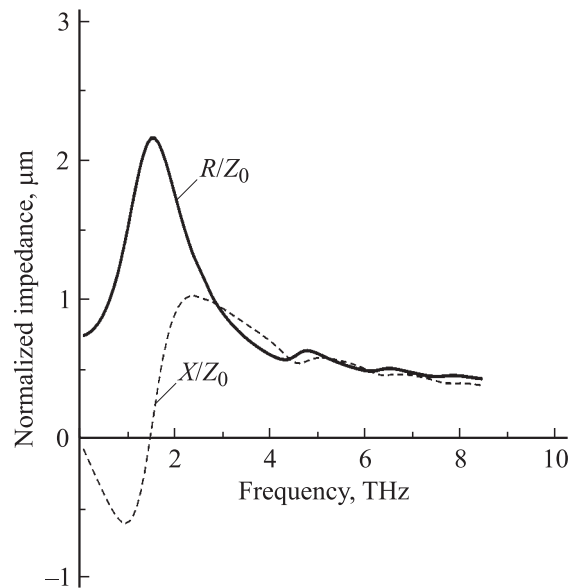


Figure 2. Impedance of the slot diode with two-dimensional electron channel vs. frequency.

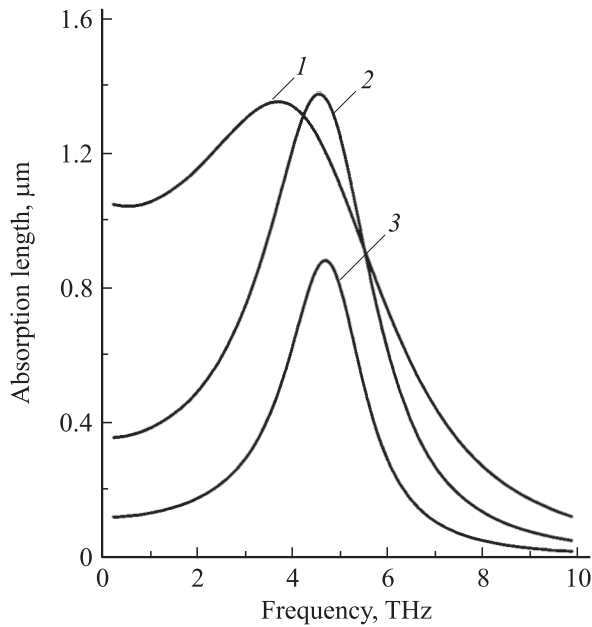


Figure 3. Absorption length of the slot diode with parameters: $N = 3 \cdot 10^{12} \text{ cm}^{-2}$, $w = 0.1 \mu\text{m}$, $\epsilon_s = 13.88$, $m^* = 0.042m_0$ as a function of the frequency for different electron scattering rates: $\nu = 2 \cdot 10^{13} \text{ s}^{-1}$ (curve 1); $7 \cdot 10^{12} \text{ s}^{-1}$ (curve 2); $2.3 \cdot 10^{12} \text{ s}^{-1}$ (curve 3).

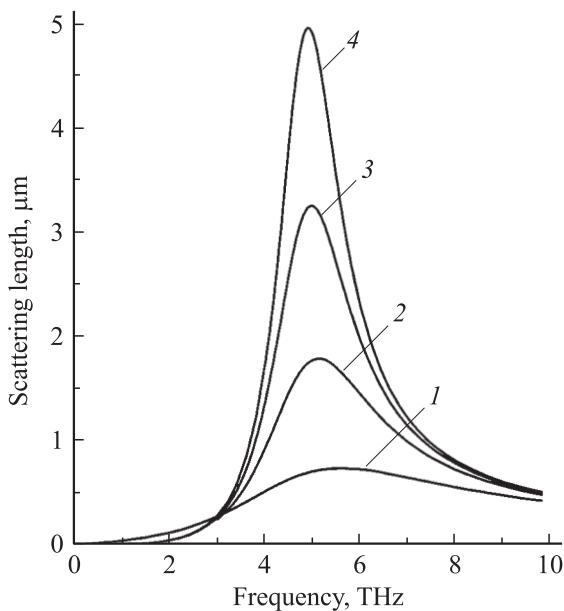


Figure 4. Scattering length of the slot diode as a function of the frequency for different electron scattering rates: $\nu = 2 \cdot 10^{13} \text{ s}^{-1}$ (curve 1); $7 \cdot 10^{12} \text{ s}^{-1}$ (curve 2); $2.3 \cdot 10^{12} \text{ s}^{-1}$ (curve 3); $\nu = 0$ (curve 4). Other parameters of the diode are the same as those in Fig. 3.

of plasma oscillations even with no electron scattering in the channel. The width of the scattering resonance in the absence of electron scattering (see curve 4 in Fig. 4) is entirely of the radiative damping origin. To minimize an

error arisen from the non-resonant background contribution, we estimate the radiative damping of plasmons, γ_{rad} , as the half width at half magnitude (HWHM) in the low-frequency slope of the scattering resonance curve for $\nu = 0$ (curve 4 in Fig. 4), which yields $\gamma_{\text{rad}} = 4.27 \cdot 10^{12} \text{ s}^{-1}$. Then the electron scattering contribution to the resonance linewidth can be obtained as a difference between the HWHM measured in the low-frequency slope of the scattering resonance at any given $\nu \neq 0$ (or, which yields the same result, in the high-frequency slope of the corresponding absorption resonance) and the radiative damping. The scattering length at the plasma resonance monotonically grows with decreasing the electron scattering rate, while the resonant absorption exhibits maximum when the dissipative broadening (caused by the electron scattering in the channel) of the resonance linewidth becomes equal to the radiative broadening (curve 2 in Fig. 3 corresponds to this case). Both the weaker as well as stronger electron scattering result in smaller resonant absorption. Note that under the condition of maximal absorption the scattering length of the diode is approximately equal to its absorption length, which puts the limit of the absorption-to-scattering length ratio of the diode close to unity.

We conclude that a slot diode with two-dimensional electron channel provides a resonant circuit at terahertz frequencies that effectively couples to external electromagnetic radiation with the loaded Q -factor exceeding unity even at room temperature. We also claim that the diode high-frequency resistance may be measured from contactless measurements of the characteristic electromagnetic lengths of the diode.

This work has been supported by the Russian Foundation for Basic Research through Grant 03-02-17219 and by the Russian Academy of Sciences Program „Novel Materials and Structures“. W.K. acknowledges a support from CNRS-programm „New THz Emitters and Detectors“, Region Languedoc Roussillon, and from the French Ministry of the Research and New Technologies program ACI „Nanosciences and Nanotechnologies“.

References

- [1] M.S. Shur, V. Ryzhii. In: *Terahertz Sources and Systems*, ed. by R. Miles, P. Harrison and D. Lippens (Dordrecht, Kluwer, 2001) p. 169.
- [2] M. Dyakonov, M. Shur. *Phys. Rev. Lett.*, **71**, 2465 (1993).
- [3] M. Dyakonov, M. Shur. *IEEE Trans. Electron. Dev.*, **43**, 380 (1996).
- [4] M.S. Shur, J.-Q. Lü. *IEEE Trans. Microwave Theory and Techniques*, **48**, 750 (2000).
- [5] W. Knap, V. Kachorovskii, Y. Deng, S. Rumyantsev, J.-Q. Lü, R. Gaska, M.S. Shur, G. Simin, X. Nu, M. Asif Khan, S.A. Saylor, L.C. Brunel. *J. Appl. Phys.*, **91**, 9346 (2002).
- [6] W. Knap, Y. Deng, S. Rumyantsev, J.-Q. Lü, M.S. Shur, C.A. Saylor, L.C. Brunel. *Appl. Phys. Lett.*, **80**, 3433 (2002).
- [7] X.G. Peralta, S.G. Allen, M.C. Wanke, N.E. Harff, J.A. Simmons, M.P. Lilly, J.L. Reno, P.J. Burke, J.P. Eisenstein. *Appl. Phys. Lett.*, **81**, 1627 (2002).

- [8] W. Knap, Y. Deng, S. Romyantsev, M.S. Shur. Appl. Phys. Lett., **81**, 4637 (2002).
- [9] V.V. Popov, O.V. Polischuk, T.V. Teperik, X.G. Peralta, S.J. Allen, N.J.M. Horing, M.C. Wanke. J. Appl. Phys., **94**, 3556 (2003).
- [10] V.V. Popov, T.V. Teperik, O.V. Polischuk, X.G. Peralta, S.L. Allen, N.J.M. Horing, M.C. Wanke. Phys. Solid State, **46**, 153 (2004).
- [11] Y. Deng, R. Kersting, J. Xu, R. Ascazubi, Xi-C. Zhang, M.S. Shur, R. Gaska, G.S. Simin, M. Asif Khan, V. Ryzhii. Appl. Phys. Lett., **84**, 70 (2004).
- [12] W. Knap, J. Lusakowski, T. Parenty, S. Bollaert, A. Cappy, V.V. Popov, M.S. Shur. Appl. Phys. Lett., **84**, 2331 (2004).
- [13] A.V. Antonov, V.I. Gavrilenko, E.V. Demidov, S.V. Morosov, A.A. Dubinov, J. Lusakowski, W. Knap, N. Dyakonova, E. Kaminska, A. Piotrowska, K. Goloszewska, M.S. Shur. Phys. Solid State, **46**, 146 (2004).
- [14] P.J. Burke, I.B. Spielman, J.P. Eisenstein, L.N. Pfeiffer, K.W. West. Appl. Phys. Lett., **76**, 745 (2000).
- [15] V. Ryzhii, A. Satou, M.S. Shur. J. Appl. Phys., **93**, 10 041 (2003).
- [16] R.G. Newton. *Scattering theory of waves and particles* (N.Y., McGraw-Hill, 1966).
- [17] J. Alsmeier, E. Batke, J.P. Kotthaus. Phys. Rev. B, **40**, 12 574 (1989).

Редактор Т.А. Полянская